Glycerol carbonate and solketal carbonate as circular economy bricks for supercapacitors and potassium batteries

Proceedings of Eurodrying'2019
Torino, Italy, July 10-12, 2019

Paper 48

A DESIGN SPACE APPROACH FOR THE FREEZING STEP OF FREEZE DRYING: CONSIDERATIONS FOR PROCESS PERFORMANCE AND PROTEIN STABILITY

Andrea Arsiccio*, *Roberto Pisano

Department of Applied Science and Technology, Politecnico di Torino
Corso duca degli Abruzzi 24, 10129 Torino, Italy
Email: roberto.pisano@polito.it

Abstract
The freezing step plays a fundamental role in the freeze drying process, as it determines product morphology and overall efficiency. The current approach to the selection of freezing conditions is however non-systematic, resulting in poor process control. Here we show how mathematical models, and a design space approach, can guide the selection of the optimal freezing protocol, focusing on both process performance and protein stability.

***Keywords**: freezing, freeze drying, design space, quality by design, protein stability*

1. Introduction

The ice crystal size which is formed during the freezing step of freeze drying is crucial for the overall process, as it is linked to stability of the active ingredient, and also corresponds to the pore dimension of the final product. Generally, a faster cooling rate results in smaller ice crystals, and therefore larger ice-water interface (Kasper and Friess, 2011). The ice crystals size is also dramatically influenced by the nucleation temperature, with a higher nucleation temperature resulting in larger crystals (Capozzi and Pisano, 2018).

The ice-water interface has been identified as a major cause of protein unfolding and aggregation (Bhatnagar *et al*,. 2008). Hence, it is clear that the ice crystals size is a critical parameter when protein stability is concerned. In addition, the pore dimension of a freeze dried product is also intimately tied to process efficiency and product quality. A large pore size promotes removal of water by sublimation, decreasing the primary drying time, and results in a lower temperature within the product being dried, minimizing the risk of collapse.

In spite of the importance of the subject, the selection of freezing conditions is currently non-systematic, and this is not in line with the guidelines issued by regulatory agencies, that emphasize the necessity for a Quality by Design (QbD) approach (US Food and Drug Administration, 2002). QbD prioritizes process understanding and control in order to guarantee the desired characteristics of the final product (Yu *et al.*, 2014).

To fill this gap, here we will demonstrate how the design of the freezing step of freeze drying could benefit from the QbD concept. In particular, a design space approach will be used. Design space is a tool that may be used in the QbD process to provide useful information about the effect of input variables on output critical parameters. In a previous work, a design space showing the effect of freezing conditions on the efficiency of primary drying was calculated (Arsiccio and Pisano, 2018). Here, the same approach will be extended to the problem of protein stability, that was not considered in the abovementioned study. The objective is to guide the selection of freezing conditions, that allow optimal preservation of proteins biological activity, while ensuring process economic efficiency at the same time.

2. Material and methods

Simulation approach

Freezing of a protein-based active ingredient was considered in this work, and a two-state unfolding process N ⇆ U of a protein, from the native (N) to denatured (U) state, was hypothesized.

For a reversible two-step process, the following system of differential equations can be written

$$\frac{d[U]}{dt} = -k_f[U] + k_u[N]$$
$$\frac{d[N]}{dt} = +k_f[U] - k_u[N] \quad (1)$$

where the kinetic constants k_f and k_u depend on temperature T, osmolyte concentration c and solution viscosity μ,

$$k_u(T, c, \mu) = A\frac{\mu_0}{\mu}e^{-\Delta G^{N-TS}/RT}$$
$$k_f(T, c, \mu) = A\frac{\mu_0}{\mu}e^{-\Delta G^{U-TS}/RT} \quad (2)$$

A is a constant, and μ_0 the viscosity at some reference conditions. If the process is irreversible, $k_f = 0$. The free energy change ΔG associated to the passage from native or denatured state, and the transition state (TS), is given by

$$\Delta G^{X-TS}(T, c) = \Delta H_0^{X-TS} - T\Delta S_0^{X-TS} + \Delta C_p^{X-TS}[T - T_0 - T\ln T/T_0] + m^{X-TS}c \quad (3)$$

with X=N, U. ΔH_0, ΔS_0 and ΔC_p are the enthalpy, entropy and specific heat change at a reference temperature T_0, while the proportional coefficient m depends on the excipient considered.

In the present work, realistic values were chosen for all the parameters related to protein stability, but with no reference to any specific protein. These values were also varied among different simulations, to cover an as wide as possible range of protein folding stabilities. The results presented in the following aim, therefore, to have general validity, qualitatively describing a variety of situations that may occur during the freezing of a protein formulation.

First of all, the ice crystal size dimension was calculated using a mechanistic model (Arsiccio *et al.*, 2017), with the iterative procedure described in Arsiccio *et al.* (2018). Freezing of a 5% w/w sucrose formulation with a 150:1 sucrose to protein mole ratio was considered. During the simulations, the shelf temperature was linearly decreased from 293 to 233 K, with varying cooling rates over the range 0.1-1 K min^{-1}. The nucleation temperature was also varied in the range 248-265 K, and an 8x8 matrix of cooling rate x nucleation temperature conditions was considered to build the design space, as it was done in Arsiccio and Pisano (2018). The average ice crystal size d_p within the product was computed for each point of this matrix, and the resulting ice-water surface area S was computed from,

$$S = \frac{4m}{d_p\rho} \quad (4)$$

where ρ is the ice density, m the initial mass of water in the vial, and the assumption was made that ice crystals are cylinder-shaped.

The increase in sucrose concentration as a result of the freezing process was computed using the data reported in Young and Jones (1949), while the solution viscosity as function of temperature and excipient concentration was calculated using the scaled Arrhenius equation (Longinotti and Corti, 2008).

For the estimation of ΔG, values of 0.2 kJ kmol^{-1} K^{-1}, 3 kJ kmol^{-1} K^{-1} and 295 K were considered for ΔS_0, ΔC_p and T_0, respectively. By contrast, the values of ΔH_0 and m were varied from simulation to simulation, to sample different situations of protein bulk stability. The kinetic constants k_u and k_f were then computed assuming $\Delta G^{N\text{-}TS} = 1.5\ \Delta G$ and $\Delta G^{U\text{-}TS} = 0.5\ \Delta G$, while the constant A was again changed from simulation to simulation.

Equations 1 were finally integrated in Matlab R2017a, using a 0.1 s time-step. The percentage of unfolded protein as a result of bulk denaturation could therefore be computed. However, surface-induced denaturation may also occur, as a result of adsorption to the ice-water interface. From equation 4 it was possible to calculate the final extension S of the ice-water surface interface, while its change during the process was estimated from

$$S_i(t) = S\ \frac{c_{w,end}}{c_w(t)} \tag{5}$$

where $c_{w,end}$ is the water mass fraction at the end of freezing, while c_w is its current value.

The percentage of surface-denatured molecules was computed assuming that the protein behavior was perturbed whenever it was closer than d_i = 4 nm to the ice surface. To determine the number n_p of adsorbed protein molecules (having molar mass M_p and molecular volume V_p), the following system of equations was solved,

$$\begin{aligned} n_w M_w &= c_w(n_w M_w + n_p M_p + n_s M_s) \\ S_i d_i &= V_w n_w + V_p n_p + V_s n_s \end{aligned} \tag{6}$$

where n_s and n_w are the number of adsorbed sucrose and water molecules, respectively, while M_w, M_s and V_w, V_s are their molar masses and molecular volumes. It was assumed that the ratio n_s/n_p was the same as in the bulk, i.e., 150. A model protein with M_p = 7000 g mol^{-1} and V_p = 6 nm^3 was considered for the simulations. It was also assumed that the surface-driven denaturation of the protein occurred with no thermodynamic barrier. This means that 50% of the adsorbed protein molecules are in the unfolded state.

For the simulations, both the completely reversible situation, and the completely irreversible one were considered. The parameters used for the simulations performed in this work are listed in Table 1.

Table 1. Details of simulations performed

	ΔH_0, kJ mol^{-1}	m, kJ mol^{-1} M^{-1}	A, s^{-1}	Reversible
1	80	4	$2\cdot10^2$	yes
2	60	1	$2\cdot10^2$	yes
3	100	4	$2\cdot10^1$	no
4	80	4	$2\cdot10^2$	no

The simulated conditions were chosen so as to explore a wide range of bulk protein stability (different ΔH_0), while keeping fixed the behavior at the ice surface. Simulations 1 and 3 correspond to proteins that are significantly more stable in bulk solution than at the surface. By contrast, the model proteins described in simulations 2 and 4 are unstable in bulk, and tend to unfold quickly at the low temperature experienced during freezing.

The crystal size d_p of the frozen product also equals the pore dimension of the dried cake, provided that no collapse occurs. In turn, the pore dimension determines the mass transfer resistance to vapor flow during primary drying, and, therefore, primary drying time t_d and maximum temperature reached during this phase T_{max}. Thus, in order to assess the effect of ice crystal size on t_d and T_{max}, a simple 1-dimensional model was used (Fissore and Pisano, 2015). The primary drying model was implemented in Matlab and solved using the finite differences approach, with a 60 s timestep.

Experimental Validation

Some experimental tests were performed to validate the simulation results. Myoglobin was selected as model protein because it is characterized by a high cold denaturation temperature (10 °C at pH 3.7 according to Privalov, 1997). The protein was obtained from Sigma Aldrich (Milan, Italy) and dissolved in 10 mM sodium citrate buffer pH 3.7. Myoglobin concentration was adjusted to either 0.1

or 0.2 mg/ml, and the presence of the surfactant Tween 80 (Sigma Aldrich, Milan, Italy) at 0.01% w/v was also considered for this study. All the solutions were prepared using ultrapure water (Fresenius Kaby, Verona, Italy), and filtered using 0.2 µm filters. To assess the effect of different ice-water surface areas on protein stability, two different freezing protocols were used. In the first one, samples were frozen by immersing vials (0.5 ml Screw Cap GeNunc Storage Vials, HDPE, Sterile, Thermo Fischer Scientific, Rochester, NY, USA) into liquid nitrogen for 5 min, and then thawed in air at room temperature. In the second protocol, 2 ml of each sample were filled into 4R 16x45 mm vials (Nuova Ompi glass division, Stevanato Group, Piombino Dese, Italy), partially stoppered with silicon stoppers (West Pharmaceutical Services, Milan, Italy) and loaded onto the shelves of a freeze dryer (Revo, Millrock Technology, Kingston, NY, USA) where shelf-ramped freezing was performed at 1 °C/min cooling rate, from 10 to -35 °C. Also in this case, samples were thawed in air at room temperature. In the case of quench cooling in liquid nitrogen, a large ice-water surface area should be formed, while the biggest ice crystals should be obtained at the lowest cooling rate used (1 °C/min). In all cases, three freeze-thaw cycles were performed, and samples were analyzed both after the first and the third cycle. Before the analyses, the protein solutions were centrifuged at 13000 rpm for 5 min (Heraeu Megafug 8 Centrifuge Series, Thermo Fisher Scientific, Milano, Italy), and the percentage of aggregates was thereafter calculated from the decrease in protein concentration (UV detection at 410 nm) after centrifugation. Optical density (OD) was measured against a solvent-matched reference using a 6850 UV/VIS spectrophotometer (Jenway, Stone, Staffordshire, UK).

3. Results and discussion

In this work, the behavior of a model protein during a freezing process in vials has been simulated. A typical output of a simulation is shown in Fig. 1. Before the nucleation event, the solution viscosity μ is too low to significantly hinder the conformational changes of the protein, and the kinetic constants show moderately high values. Immediately after the nucleation, i.e., after approximately 0.7 h in the case of Fig. 1, the excipient concentration c increases sharply because of the formation of ice crystals (Fig. 1a), and this augments the bulk stability of the protein. This is evident from Fig. 1b, where the free energy change ΔG is shown both including (red curve) or neglecting (black curve) the effect of the osmolyte. In this case, the effect of the excipient is stabilizing (positive m-value), as it shifts the free energy of unfolding to larger values. While the two curves are almost superimposed before nucleation, they clearly split apart as soon as the first ice crystals are formed. The viscosity increases as well (Fig. 1a), kinetically hindering any protein movement. As a consequence, the kinetic constants k_u and k_f drop to very low values (Fig. 1d). Surface-driven denaturation becomes therefore dominant after nucleation, and a not negligible amount of protein molecules adsorb to the ice surface, potentially undergoing conformational changes (Fig. 1c).

The resulting fraction of unfolded (U) and native (N) protein molecules as function of freezing time is shown in Fig. 1e-f. In the case of Fig. 1e, simulation 1 in Table 1 is considered. In this case, the protein is stable in bulk, as the folding rate constant (k_f) is remarkably larger than the unfolding (k_u) one (see Fig. 1d). Therefore, the unfolded protein molecules convert back almost immediately to the native state, and no notable unfolding occurs before nucleation. In this case, surface-driven denaturation prevails.

On the other hand, if simulation 4 in Table 1 is considered (Fig. 1f), a significant percentage of the protein undergoes conformational changes before nucleation, and the denaturation induced by the ice surface is negligible. As evident from this first example, an important role is therefore played by the ratio between bulk and surface stability. A design space approach was therefore used to further investigate the implications of this observation.

In simulations 1 and 3 of Table 1, surface-induced unfolding is dominant, while it becomes negligible in the case of simulations 2 and 4. As we are not interested in the absolute value of unfolded protein molecules in each configuration, the graphs will show the percentage of unfolded molecules (U), normalized by the maximum value observed in each design space (U_{max}). This will allow an easier comparison between different conditions.

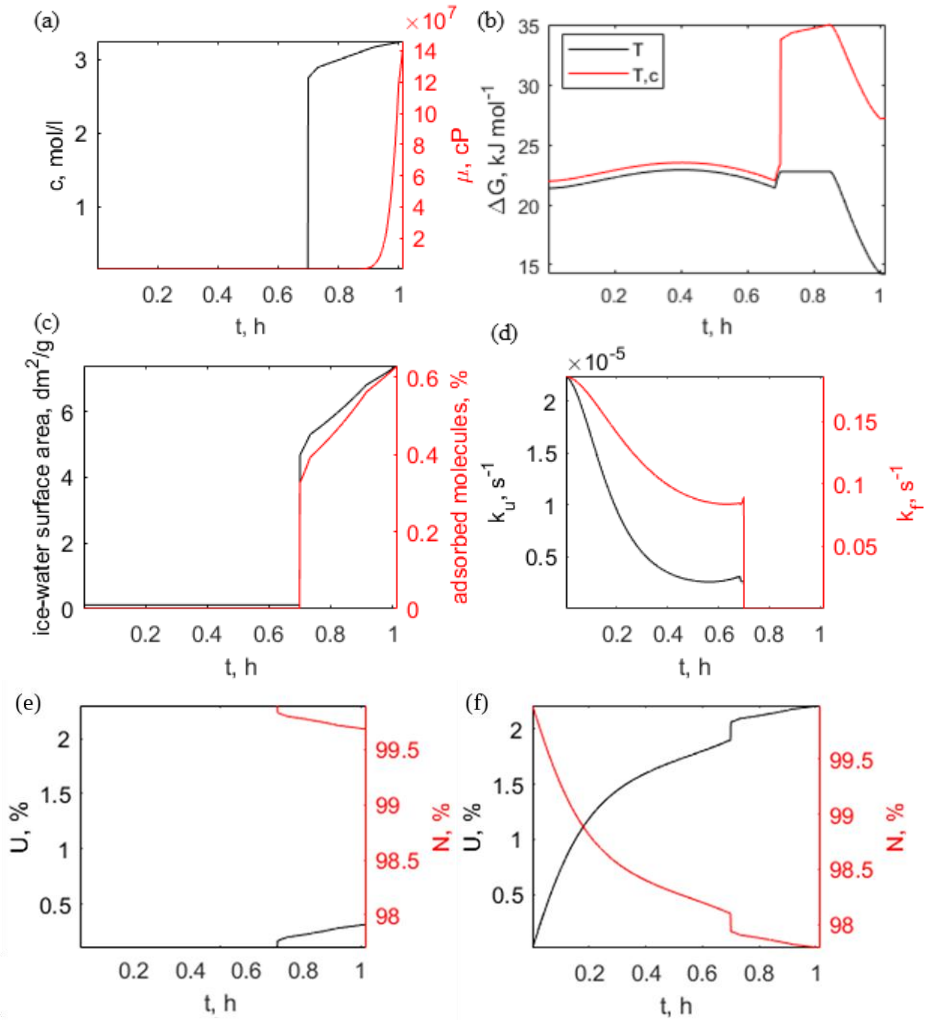

Fig. 1. Typical output of a simulation, for 1 °C min^{-1} as cooling rate and 260 K as nucleation temperature. Evolution of (a) sucrose concentration c and solution viscosity μ, (b) free energy change ΔG including (red curve) or neglecting (black curve) the effect of the osmolyte, (c) extension of the ice-water surface area (in dm^2/g, using the solvent mass as reference) and percentage of adsorbed molecules, (d) rate constants k_u and k_f as function of the freezing time, for the conditions of simulation 1 in Table 1. Percentage of unfolded (U) and native (N) protein molecules as function of the freezing time, in the case of (e) simulation 1 and (f) simulation 4.

In line with previous considerations, the design space for simulation 1 (Fig. 2a) shows that the worst condition for protein stability (U/U_{max} = 100%) corresponds to the region of high cooling rates and low nucleation temperature. As mentioned in the Introduction, small ice crystals are formed in these conditions, that result in a large ice-water surface, as shown by the red isocurves in Fig. 2. It is evident that the greater the extension of the ice interface is, the more the protein unfolds. In these conditions surface-induced denaturation prevails, and the optimal process should maximize the ice crystal size.

If the protein has a reduced stability in bulk, as in simulation 2, surface-induced denaturation becomes negligible. In this case (Fig. 2b), a low cooling rate results in the highest degree of protein unfolding. This happens because the lower the cooling rate is, the longer the solution viscosity is low enough to allow fast conformational changes. Therefore, if a protein with low bulk stability is considered, a high cooling rate may be beneficial, as it would result in shorter freezing times and earlier cryoconcentration.

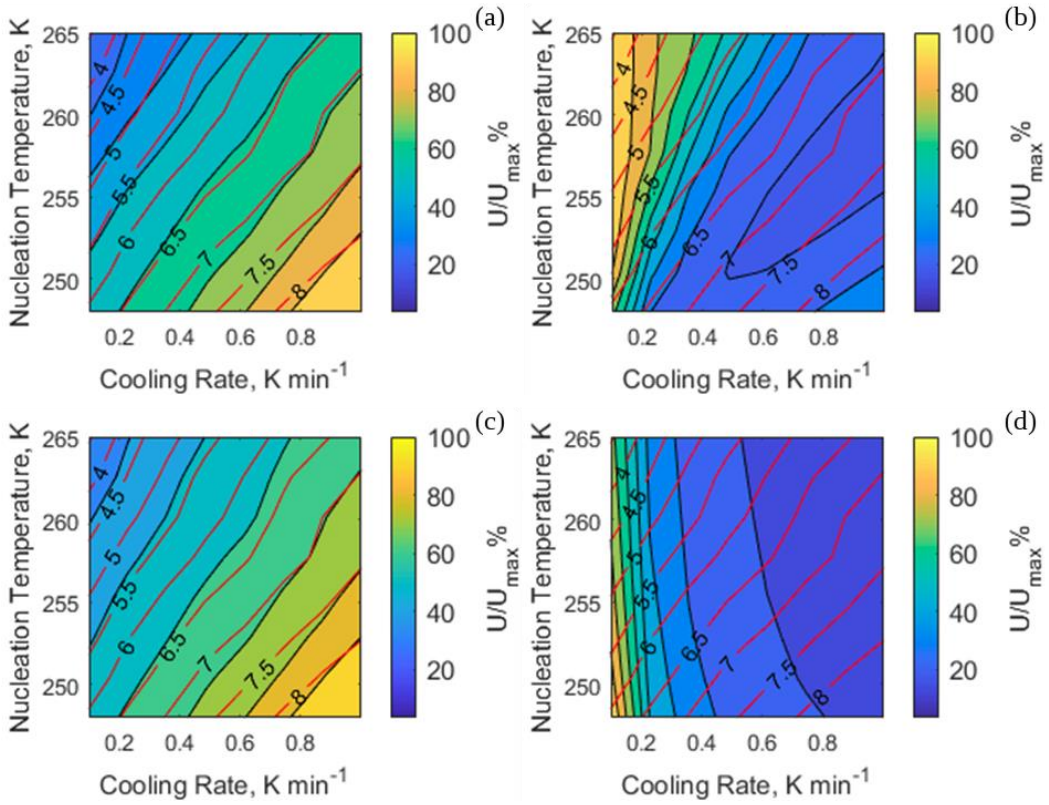

Fig. 2. Design space showing the stress for the protein (percentage of unfolded protein, normalized by its maximum value in the design space), for simulations 1 (a), 2 (b), 3 (c) and 4 (d) in Table 1. The red isocurves identify the conditions resulting in the same total extension of the ice-water surface area, reported in dm^2/g (solvent mass is used as reference) on the curves.

Similar considerations apply to the case of irreversible conformational changes. In the case of simulation 3 (Fig. 2c), surface-driven unfolding is again dominant and slow cooling rates/high nucleation temperature conditions should be preferred. On the other hand, if the denaturation process in the bulk solution is thermodynamically and kinetically favored, as in simulation 4 (Fig. 2d), the extension of the ice interface is not a crucial parameter, while the duration of the freezing process should be strictly controlled, and a cryoconcentrated matrix should be formed as quickly as possible.

The first scenario herein described, that primarily ascribes protein denaturation to the increase of the ice-water interface, is well-documented in the literature. For instance, using LDH as model protein, a remarkable loss of activity was observed in frozen systems, while no degradation was detected in concentrated solutions at the same temperature and composition, but without ice (Bhatnagar *et al.*, 2008). Similarly, phosphofructokinase (PFK), lactate dehydrogenase (LDH), glutamate dehydrogenase (GDH), interleukin-1-receptor antagonist (IL-1ra), tumor necrosis factor binding protein (TNFbp), and ciliary neurotropic factor (CNTF) were observed to form a large amounts of insoluble precipitates when quench cooled in liquid nitrogen, while a smaller cooling rate caused less precipitation (Chang *et al.*, 1996). Also, the addition of small amount of surfactant could effectively prevent the observed precipitation.

These results suggest that surface-driven denaturation at the ice-water interface is dominant for many proteins, and indicate that the behaviour described in Fig. 2a and 2c is commonly observed in experiments. By contrast, it is not easy to find in the literature reports of proteins that behave according to Fig. 2b and 2d. This occurs because most of the proteins commonly used for this type of experiments show a quite high bulk stability, and are unlikely to exhibit any significant denaturation before the onset of ice formation. In contrast, the model protein selected in this work, namely, myoglobin, is extremely sensitive to cold denaturation, especially at the low pH (3.7) selected for this study (Privalov, 1997). In Fig. 3 the percentage of myoglobin recovery after freeze thawing is shown, as measured from the OD at 410 nm. As can be observed, the fastest freezing protocol, i.e., quenching

in liquid nitrogen, resulted in the highest protein recovery. The addition of Tween 80 did not improve the situation, but actually resulted in enhanced aggregation, probably because the surfactant promoted protein denaturation. This suggests that the surface contribution was negligible, while bulk denaturation was dominant, in line with the design space shown in Fig. 2b and 2d. Therefore, both the scenarios identified by the simulations can be experimentally observed, and this indicates that the simulation approach can capture at least the main features of protein stability during freezing.

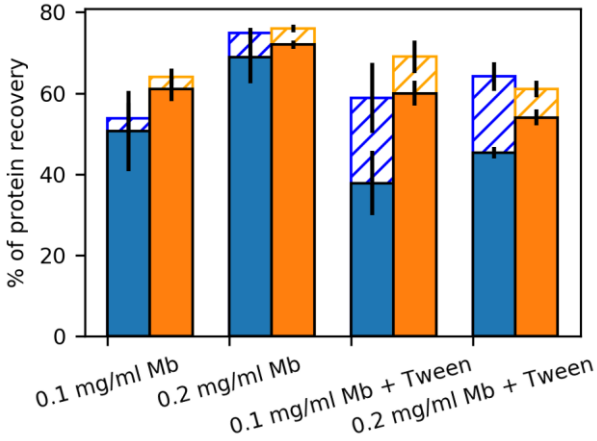

Fig. 3. Percentage of myoglobin recovery after 1 (dashed bars) and 3 (colored bars) freeze thawing cycles performed at 1 °C min^{-1} (blue bars) or in liquid nitrogen (orange bars).

In addition to protein stability, process efficiency should also be considered. As previously mentioned, the ice crystal size corresponds to the pore dimension that is formed within the dried product, provided that no collapse occurs. A large pore size reduces the resistance to mass transfer, and promotes the sublimation process, thus resulting in shorter drying times. At the same time, a smaller resistance to water vapor transfer through the dried layer is associated with a lower product temperature, and therefore reduced risk of product collapse. The impact of the freezing process on the subsequent drying step is schematized in Fig. 4, where the primary drying time t_d and maximum product temperature T_{max} have been calculated as function of cooling rate and nucleation temperature.

It is evident that a small cooling rate and a high nucleation temperature are beneficial for process efficiency. This choice of freezing conditions also results in the best preservation of protein activity, if proteins with high bulk stability are considered. However, this is not true anymore when the protein being dried is extremely prone to cold denaturation, as for myoglobin. In this case, a high cooling rate would preserve biological activity the most, and a trade-off should be achieved between efficiency and product quality. Lastly, it should be taken into account that in a common freezing process, it is not possible to have direct control on the nucleation temperature, and some interaction has even been observed between this variable and the cooling rate, with slower cooling rates promoting a higher degree of supercooling and therefore a faster freezing rate (Kasper and Friess, 2011). Some controlled nucleation techniques have been developed (Pisano, 2019), but in this case temperatures above the onset of spontaneous nucleation must be used. This means that only a portion of the design space shown in this work can generally be experimentally sampled, and suggests that further work needs to be done to achieve a complete control of the freezing process. This will be the subject of future investigations.

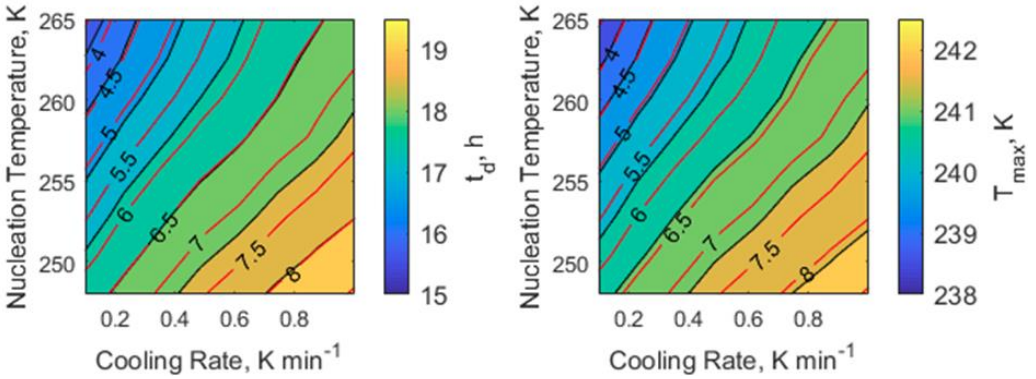

Fig. 4. Design space showing the primary drying time t_d and the maximum temperature T_{max} reached within the product. A fluid temperature and chamber pressure of 253 K and 10 Pa, respectively, have been considered for simulations of the primary drying step.

4. Conclusions

Using the proposed approach, based on mathematical modeling and the use of the design space, two opposite situations have been encountered. If the protein is more stable in the bulk solution than at the ice interface, the freezing process should be designed so as to result in a small ice-water surface area. This is also beneficial for the subsequent primary drying step, that can be completed in a shorter time and with reduced risk of product collapse. On the contrary, a high cooling rate, resulting in a fast immobilization of the protein in a glassy matrix, should be preferred if the protein being frozen is poorly stable in solution. This last scenario, suggested by *in silico* modelling, is confirmed by experimental results for myoglobin as model protein.

References

Arsiccio A., Barresi A.A. and Pisano R., 2017, Prediction of ice crystal size distribution after freezing of pharmaceutical solutions, *Cryst. Growth Des.* **17**, 4573-4581.

Arsiccio A., Barresi A.A., De Beer T., Oddone I., Van Bockstal P-J. and Pisano R., 2018, Vacuum induced surface freezing as an effective method for improved inter- and intra-vial product homogeneity, *Eur. J. Pharm. Biopharm.* **128**, 210-219.

Arsiccio A. and Pisano R., 2018, Application of the Quality by Design approach to the freezing step of freeze drying: Building the design space, *J. Pharm. Sci.* **107**, 1586-1596.

Bhatnagar B.S., Pikal M.J. and Robin H.B, 2008, Study of the individual contributions of ice formation and freeze-concentration on isothermal stability of lactate dehydrogenase during freezing, *J. Pharm. Sci.* **97**, 798-814.

Capozzi L.C. and Pisano R., 2018, Looking inside the black box: Freezing engineering to ensure the quality of freeze-dried biopharmaceuticals, *Eur. J. Pharm. Biopharm.* **129**, 58-65.

Chang B.S., Kendrick B.S. and Carpenter J.F., 1996, Surface-induced denaturation of proteins during freezing and its inhibition by surfactants, *J. Pharm. Sci.* **85**, 1325-1330.

Fissore D, and Pisano R., 2015, Computer-aided framework for the design of freeze-drying cycles: optimization of the operating conditions of the primary drying stage. *Processes* **3**, 406-421.

Kasper J.C. and Friess W.F., 2011, The freezing step in lyophilization: Physico-chemical fundamentals, freezing methods and consequences on process performance and quality attributes of biopharmaceuticals. *Eur. J. Pharm. Biopharm.* **78**, 248-263.

Longinotti M.P. and Corti H.R., 2008, Viscosity of concentrated sucrose and trehalose aqueous solutions including the supercooled regime, *J. Phys. Chem. Ref. Data* **37**, 1503-1515.

Pisano R., 2019, Alternative methods of controlling nucleation in freeze drying, in: "*Lyophilization of Pharmaceuticals and Biologicals. Methods in Pharmacology and Toxicology"* (K. Ward and P. Matejtschuk, Eds.), Humana Press, New York, pp. 79-111.

Privalov P.L., 1997, Thermodynamics of protein folding, *J. Chem. Thermodyn.* **29**, 447-474.

US Food and Drug Administration, Department of health and human services, 2002, Pharmaceutical cGMPs for the 21st century: A risk-based approach.

Young F.E. and Jones F.T., 1949, Sucrose hydrates. The sucrose–water phase diagram, *J. Phys. Chem.* **53**, 1334-1350.

Yu L.X., Amidon G., Khan M.A., Hoag S.W., Polli J., Raju G.K. and Woodcock J., 2014, Understanding pharmaceutical quality by design. *AAPS J.* **16**, 771-783.